Journal of Cellular Biochemistry 103:1464–1471 (2008)

Biochemical Analysis of the Interaction of Calcium With Toposome: A Major Protein Component of the Sea Urchin Egg and Embryo

Michael Hayley,[1] Ming Sun,[2] Erika F. Merschrod S,[2] Philip J. Davis,[1] and John J. Robinson[1]*

[1]Department of Biochemistry, Memorial University of Newfoundland, St John's, Newfoundland, Canada A1B 3X9
[2]Department of Chemistry, Memorial University of Newfoundland, St John's, Newfoundland, Canada A1B 3X9

Abstract We have investigated the biochemical and functional properties of toposome, a major protein component of sea urchin eggs and embryos. Atomic force microscopy was utilized to demonstrate that a Ca^{2+}-driven change in secondary structure facilitated toposome binding to a lipid bilayer. Thermal denaturation studies showed that toposome was dependent upon calcium in a manner paralleling the effect of this cation on secondary and tertiary structure. The calcium-induced, secondary, and tertiary structural changes had no effect on the chymotryptic cleavage pattern. However, the digestion pattern of toposome bound to phosphatidyl serine liposomes did vary as a function of calcium concentration. We also investigated the interaction of this protein with various metal ions. Calcium, Mg^{2+}, Ba^{2+}, Cd^{2+}, Mn^{2+}, and Fe^{3+} all bound to toposome. In addition, Cd^{2+} and Mn^{2+} displaced Ca^{2+}, prebound to toposome, while Mg^{2+}, Ba^{2+}, and Fe^{3+} had no effect. Collectively, these results further enhance our understanding of the role of Ca^{2+} in modulating the biological activity of toposome. J. Cell. Biochem. 103: 1464–1471, 2008.

Key words: calcium; toposome; membrane–membrane interaction; sea urchin

The yolk granules of sea urchin eggs and embryos occupy approximately one-third of the cytoplasmic volume. The major protein component of the granule is toposome, comprising 50% of the total yolk protein [Kari and Rottmann, 1980]. Toposome, isolated from the sea urchin *Tripneustus gratilla* or *Paracentrotus lividus* appears to be a glycoprotein composed of six identical polypeptides of 160–170 kDa in size, depending on the species [Noll et al., 1985]. Interestingly, as development proceeds the 160-kDa polypeptide is proteolytically processed, post-fertilization into smaller molecular mass species, apparently as the result of a cathepsin B-like activity, sensitive to thiol-protease inhibitors [Yokota and Kato, 1988; Scott and Lennarz, 1989; Mallya et al., 1992; Yokota et al., 2003]. Although the functional significance of this processing remains to be determined, it has been suggested that it might serve to produce variants in a cell surface protein to direct morphogenic cell movements and generate epigenetic diversity [Noll et al., 1985; Matranga et al., 1986]. In addition to the yolk granule, toposome is also localized to the embryonic cell surface [Gratwohl et al., 1991] and has been identified as a molecule mediating cell–cell adhesion in the developing embryo [Noll et al., 1981; Noll et al., 1985; Matranga et al., 1986; Cervello et al., 1992].

In a previous study using both purified yolk granules and liposomes, we have characterized toposome-driven, membrane–membrane interactions [Perera et al., 2004]. This work has recently been extended with the analysis of calcium–toposome interaction [Hayley et al.,

Grant sponsor: Natural Sciences and Engineering Research Council of Canada; Grant sponsor: Canada Foundation for Innovation ; Grant sponsor: Industrial Research and Innovation Fund; Grant sponsor: Natural Sciences Research Council of Canada.

*Correspondence to: John J. Robinson, Department of Biochemistry, Memorial University of Newfoundland, Elizabeth Ave, St John's, Newfoundland, Canada A1B 3X9. E-mail: johnro@mun.ca

Received 17 May 2007; Accepted 10 July 2007

DOI 10.1002/jcb.21531

2006a]. This cation was found to induce two calcium-concentration dependent structural transitions in toposome: a secondary structural change occurred with an apparent k_d (calcium) of 25 μM and this was followed by a tertiary structural change with an apparent k_d (calcium) of 240 μM. Interestingly, the first structural change was required to facilitate toposome binding to bilayers while the second structural change correlated with toposome-driven, membrane–membrane interaction. These results provide a structural basis for the previously described toposome-mediated, cell–cell adhesion in the sea urchin embryo [Noll et al., 1985; Matranga et al., 1986; Cervello et al., 1992]. In another study, we have defined the nature of the association of toposome with the bilayer using ^{2}H-NMR [Hayley et al., 2006b]. The results of this study suggest that toposome interacts peripherally with the membrane and this interaction occurs in the presence of 100 μM calcium and is not further modulated by increased concentrations of this cation. These results correlate well with those from the previous study examining calcium–toposome interaction. Furthermore, the NMR study clearly demonstrated that the calcium-induced, tertiary structural change in toposome did not further modulate protein–membrane interactions. Collectively, these studies provide a mechanistic basis for the known cell–cell adhesive activity of toposome in the sea urchin embryo.

In the study reported here, we have utilized atomic force microscopy (AFM), thermal denaturation and protease digestion analyses to further characterize calcium–toposome interactions. In addition, we have probed the specificity of the calcium-binding sites on toposome. Collectively, our results provide further evidence for the calcium-induced structural changes in toposome and suggest that under physiological conditions, the function(s) of toposome is regulated by calcium.

MATERIALS AND METHODS

Preparation of Yolk Granule Protein Extracts and Fractionation by Ion Exchange Chromatography

Strongylocentrotus purpuratus were purchased from SeaCology, Vancouver, Canada. Eggs were harvested and washed consecutively in Millipore-filtered seawater (MFSW) and Ca^{2+}, Mg^{2+}-free seawater (CMFSW). Preparation of the yolk granule protein extract followed the procedure described previously with some modifications [Perera et al., 2004]. Washed eggs were suspended in 0.5 M KCl (pH 7.0) and homogenized in a hand-held Dounce homogenizer at 0°C. The homogenate was then fractionated by centrifugation at 400*g* for 4 min at 4°C. The supernatant was harvested and fractionated by centrifugation at 2,400*g* for 10 min at 4°C. The final pellet was resuspended in 0.5 M KCl (pH 7.0) containing 1 mM EDTA, fractionated by centrifugation at 50,000*g* for 1 h at 4°C and the supernatant retained. Aliquots of the supernatant were dialyzed against starting buffer (10 mM Tris-HCl, pH 8.0) and were loaded onto a Q-Sepharose Fast Flow column (Amersham Pharmacia, Uppsala, Sweden) that had been previously equilibrated with starting buffer. The column was washed with three column volumes of buffer to remove any unbound proteins followed by the elution of bound proteins with a NaCl step gradient (0.1–1.0 M), prepared in starting buffer. The eluted proteins were analyzed by sodium dodecyl sulfate polyacrylamide gel electrophoresis (SDS–PAGE) [Hayley et al., 2006a] as described by Laemmli [1970], and the gel stained with silver (Amersham Pharmacia, Uppsala, Sweden).

Lipid Stamping

Multilamellar vesicles used in the lipid-stamping study were prepared as follows. Dimyristoyl phosphatidyl serine was dissolved in a 2:1 chloroform:methanol solution and vortexed for 4 min. The chloroform:methanol was evaporated under N_2 and vacuum dried for 24 h. DMPS (0.1 mg/ml) was then hydrated at 45°C for 1 h in dH_2O. Aliquots, 10 μl, were then transferred onto a micropatterned, polydimethylsiloxane-stamp and allowed to dry for 5 min. The stamp was pressed directly on a glass slide and then removed upon transfer of lipids to the silicon [Hovis and Boxer, 2001]. Toposome, followed by specific concentrations of Ca^{2+}, was directly added to the lipid stamp. Imaging was performed on an MFP-3D (Asylum Research, Inc.) in contact mode using gold-coated, silicon cantilevers (Micromasch). Images are presented with minimal post-processing with a simple planefit used to correct for curvature.

Circular Dichroism Spectroscopy Measurements

Circular dichroism spectra in the far-ultraviolet region (190–230 nm) were recorded

using a Jasco-810 spectrapolarimeter. Samples were dissolved and dialysed against 20 mM Tris-HCl, pH 8.0 (unless otherwise stated) and the ellipticity at 222 nm of the protein/reagents mixture was checked to ensure that it did not exceed 1.0. A water-jacketed cell (light path = 5 mm) was used and spectra were collected between 190 and 300 nm. Baselines were established using the appropriate buffers and 12 spectra were collected for each temperature and averaged. The temperature range (5–75°C) was controlled by a CTC-345 circulating water bath. The heating rate used in all experiments was 30°C per hour. Heating rates of 15 and 60°C per hour were also used to confirm that the samples had reached thermal equilibrium (data not shown). The scanning speed of the instrument was set at 100 nm/min with normal sensitivity.

Toposome Digestion With Chymotrypsin

In a total volume of 100 μl, aliquots of toposome (5 μg), in 20 mM Tris-HCl (pH 8.0), were incubated with chymotrypsin (0.5 μg) at room temperature for 30 min. The serine protease inhibitor PMSF (1 mM) was added to stop the digestion. In digestions where calcium and/or liposomes were present, toposome was preincubated for 30 min at room temperature in the presence of calcium and/or liposomes before the addition of chymotrypsin. In digestions containing both toposome and liposomes in the presence of 500 μM calcium, toposome, and liposomes were initially incubated with 100 μM calcium for 30 min. After the 30 min incubation, the calcium concentration was increased to 500 μM and the incubation continued for an additional 30 min. Following incubation with chymotrypsin, the liposome pellets (1 mg) were harvested by centrifugation and fractionated in an 8% (w/v) SDS–PAGE gel which was stained with Coomassie Brilliant Blue R-250 [Laemmli, 1970].

Endogenous Tryptophan Fluorescence Measurements

Tryptophan fluorescence was measured at room temperature in a Shimadzu Model RF-540 spectrofluorimeter. The excitation wavelength was 287 nm and emission spectra were measured between 300 and 400 nm. In all cases, samples were dissolved in 20 mM Tris-HCl, pH 8.0 followed by the addition of the specified ion to the final concentration indicated.

Displacement Assay

Displacement assays were performed as described previously [Robinson, 1989]. Aliquots (5 μg each) of toposome were dot blotted onto a nitrocellulose membrane. The membrane was then equilibrated for 120 min at room temperature with calcium binding buffer (60 mM KCl, 10 mM imidazole-HCl, pH 6.8). Two pieces of the nitrocellulose membrane, one containing toposome and the second with no bound toposome as a control for background binding of ^{45}Ca, were incubated at room temperature for 15 min in calcium binding buffer containing ^{45}Ca (2 mCi/L). Directly after the 15 min incubation, the membranes were washed at room temperature for 5 min in 1 mM Tris-HCl (pH 7.5) or in the same buffer containing 30 μM concentrations of various salts. The membranes were then air dried and counted in 10 ml of Scinti Verse E (Fisher Scientific) in a Beckmann model LS9000 liquid scintillation counter. Background binding was corrected for by subtracting the counts of the blank membranes from those of the membranes containing bound protein.

RESULTS AND DISCUSSION

In a previous study, we demonstrated that low concentrations of calcium ($k_d = 25$ μM) induce a change in toposome secondary structure that facilitates toposome binding to bilayer lipids. In addition, we showed that higher concentrations of calcium ($k_d = 240$ μM) induced a change in tertiary structure which correlated with the ability of toposome to drive membrane–membrane interactions. In the study reported here, we have further investigated toposome-Ca^{2+} interaction. AFM was utilized to confirm our previous finding implicating the Ca^{2+}-induced, secondary structural change as the facilitator of toposome binding to bilayer lipids. Phosphatidyl serine bilayers were stamped onto glass slides and probed with toposome. In the absence of added Ca^{2+}, toposome binding to the bilayer was minimal (Fig. 1A). However, when toposome was preincubated with sufficient Ca^{2+} to induce the secondary structural change, protein binding to the bilayer occurred as evidenced by the increased number of small dots on the membrane background (Fig. 1B). The white streaks indicate that the protein remained mobile while bound to the membrane. Further increasing the Ca^{2+} concentration, to induce the tertiary

structural change, did not result in any significant increased binding of toposome to the bilayer, as seen in Figure 1C (a digital zoom at 1/10 resolution). In control experiments, minimal binding of toposome occurred in the presence of 100 or 500 μM Mg^{2+} (Fig. 1D, also a digital zoom at 1/10 resolution). This latter result clearly attests to the specificity of Ca^{2+} in modulating toposome–bilayer interaction.

Thermal denaturation experiments were performed, in the presence or absence of various concentrations of calcium, to determine if this cation modulated the stability of toposome. We chose concentrations of calcium that would induce the secondary structural change alone or both the secondary and tertiary changes. A temperature-dependent change in far-UV ellipticity was apparent in all thermal denaturation experiments (data not shown). In all the above experiments, the ellipticity at 222 nm decreased markedly with increasing temperature. At a temperature of 5°C, toposome was assumed to be fully folded. Denaturation of toposome in the presence and absence of calcium was monitored using the ellipticity values at 222 nm. The temperature dependent unfolding profile of toposome in the presence of 6 M urea was also measured. Figure 2 summarizes the thermal unfolding of toposome in the presence and absence of calcium, as well as in the presence of urea. The unfolding profile of toposome in the presence of 100 and 500 μM calcium provides further evidence for calcium-dependent structural changes in toposome. At a calcium concentration (100 μM) sufficient to induce a change in secondary structure, the protein has an increased resistance to thermal denaturation compared to toposome in the absence of calcium: at 50°C, toposome was 12.6% unfolded in the presence of 100 μM Ca^{2+} compared to 36.8% in the absence of added Ca^{2+}. Interestingly, at a calcium concentration (500 μM) that induces a change in tertiary structure, the thermal stability of toposome is increased in comparison with that seen in the absence of calcium but is less stable when compared with toposome in the presence of 100 μM calcium, 26.4% versus 12.6% unfolded at 50°C. As was expected, the thermal unfolding profile of toposome was greatly affected by the presence of 6 M urea, rendering the protein structurally unstable at much lower temperatures, 57.5%

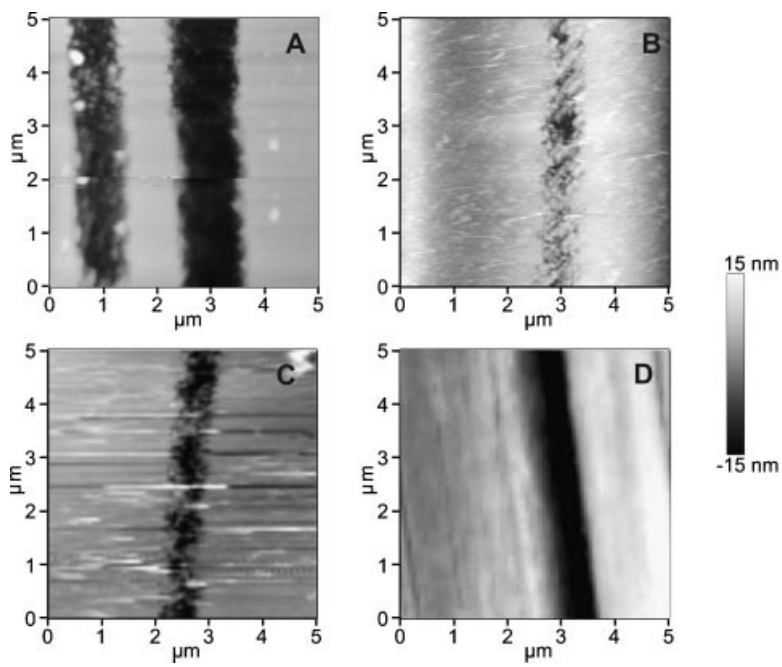

Fig. 1. Atomic force microscopic analysis of toposome binding to phosphatidyl serine bilayers in the presence of various concentrations of calcium. Representative images are presented. **A**: Toposome binding to phosphatidyl serine bilayers in the absence of exogenously added calcium. **B**: Toposome binding to phosphatidyl serine bilayers in the presence of 100 μM calcium. **C**: Toposome binding to phosphatidyl serine bilayers in the presence of 500 μM calcium. **D**: Toposome binding to phosphatidyl serine bilayers in the presence of 100 μM magnesium.

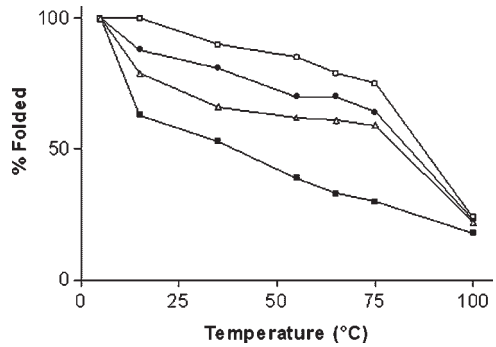

Fig. 2. Determination of the thermal unfolding profile of toposome under various conditions. Ellipticity at 222 nm was used to determine the percentage folding of the protein as a function of temperature. Reaction mixtures containing toposome and the indicated concentrations of calcium or urea were incubated at room temperature for 30 min prior to collection of the thermal unfolding data. 0 μM Ca^{2+} (△); 100 μM Ca^{2+} (□); 500 μM Ca^{2+} (●); 6 M urea (■).

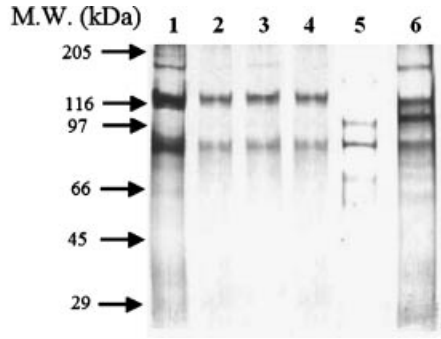

Fig. 3. SDS–PAGE analysis of the chymotryptic digestion products of toposome in the presence or absence of calcium and/or liposomes. Undigested toposome (**lane 1**). Digestion pattern for toposome in the absence of added calcium and liposomes (**lane 2**). Digestion pattern for toposome in the presence of 100 μM calcium (**lane 3**) or 500 μM calcium (**lane 4**). Digestion pattern for toposome in the presence of phosphatidyl serine liposomes and 100 μM calcium (**lane 5**) or 500 μM calcium (**lane 6**). Equal amounts of toposome were loaded in each lane and the peptides visualized by silver staining.

unfolded at 50°C. The above results agree with our previous data suggesting that toposome undergoes two distinct structural changes as a result of increasing concentrations of calcium. Interestingly, these changes in structure result in quantitatively significant differences in the thermal stability of toposome.

In the study reported here, we used limited proteolysis in the presence and absence of Ca^{2+} to examine the structure of toposome, both in the membrane-free and membrane-bound forms. Figure 3 depicts the chymotryptic digestion patterns of free and membrane-bound toposome. In the presence of chymotrypsin, the 160, 120, and 90 kDa polypeptides of toposome are all susceptible to cleavage, with complete digestion of the 160 kDa species occurring (lane 2). At a concentration of calcium (100 μM) sufficient to induce a change in the secondary structure of toposome, there was no difference in the chymotryptic digestion pattern compared to toposome in the absence of calcium (lane 2 vs. lane 3). Similarly, there was no change in the digestion pattern at a concentration of calcium (500 μM) that induced both the secondary and tertiary structural changes in the protein (lane 4). It was of interest to investigate the chymotryptic digestion pattern of toposome bound to liposomes composed of phosphatidyl serine at different concentrations of calcium. In previous experiments, we have shown that a calcium concentration of 100 μM, which is sufficient to induce the secondary structural change in toposome, facilitates quantitative binding of toposome to the bilayer [Hayley et al., 2006a]. Membrane-bound toposome ($[Ca^{2+}] = 100$ μM) showed a significant difference in the chymotryptic digestion pattern when compared to the unbound form of the protein at the same calcium concentration (lane 5 vs. lane 3). This result most likely accrues from steric hindrance resulting from the binding of toposome to the bilayer. Following toposome binding to the bilayer, the calcium concentration was increased to 500 μM and the chymotryptic digestion profile determined. In this case the digestion pattern of membrane-bound toposome was unique (lane 6). The 160 kDa species appeared refractory to digestion while the 120 and 90 kDa polypeptides were partially digested. This result confirms that Ca^{2+} can induce the tertiary structural change in toposome bound to the bilayer.

To further explore calcium–toposome interactions, we designed experiments to characterize the cation binding sites of toposome. We analyzed the effects of other cations on toposome structure. Endogenous tryptophan fluorescence emission spectra were measured by excitation at 287 nm and monitoring the emitted light between 300 and 400 nm. The maximum emission wavelength (λ_{MAX}) for toposome was 333 nm. The steady state fluorescence emission spectrum of toposome was compared in the

presence of various metal ions (Ca^{2+}, Mg^{2+}, Ba^{2+}, Cd^{2+}, Mn^{2+}, and Fe^{3+}). As shown in Figure 4, all metal ions were capable of binding to toposome. As was the case for all metal ions tested, an increase in the cation concentration resulted in an emission spectrum that was altered. Although the λ_{MAX} for toposome remained unchanged at 333 nm, each metal ion tested had a quenching effect on the amplitude of the fluorescence emitted by toposome. Each metal ion quenched the fluorescence to a different extent; $Fe^{3+} > Cd^{2+} > Ca^{2+} > Mn^{2+} > Mg^{2+} > Ba^{2+}$.

A calcium displacement assay was used to determine if the metal ions examined in the fluorescence study were binding at the calcium binding sites on toposome. The displacement assay involved the binding of ^{45}Ca to toposome, dot blotted onto a nitrocellulose membrane, followed by quantification of displacement of the

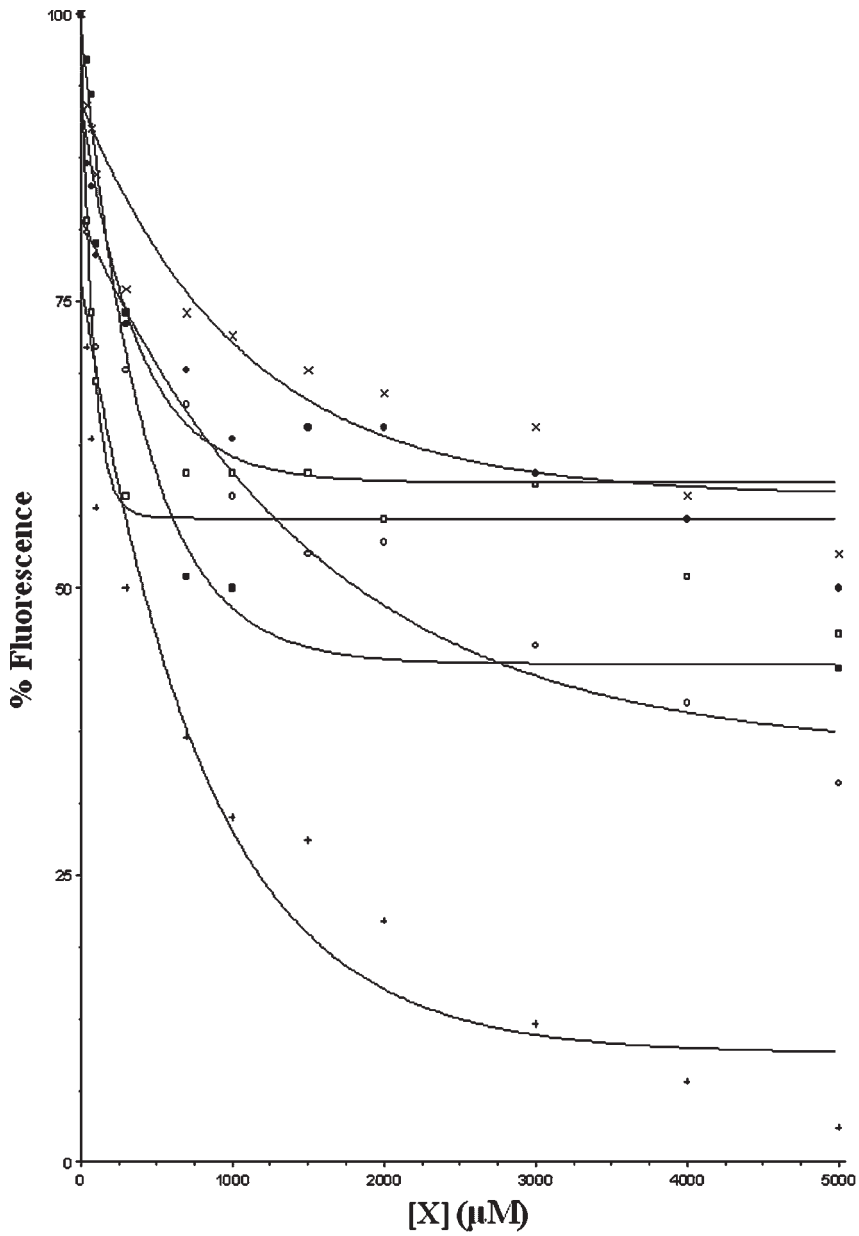

Fig. 4. Tryptophan fluorescence emission spectra of toposome in the presence of increasing concentrations of various metal ions. Aliquots of toposome were preincubated with the indicated concentrations of various metal ions for 30 min at room temperature prior to spectrophotometric analysis. Ba^{2+} (●); Ca^{2+} (■); Cd^{2+} (○); Fe^{3+} (+); Mg^{2+} (×); Mn^{2+} (□).

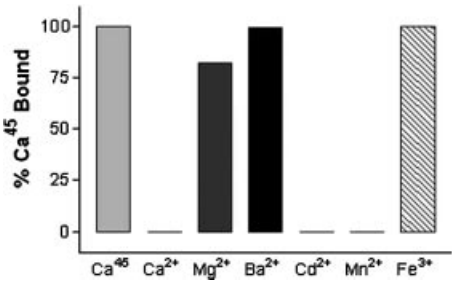

Fig. 5. Displacement of toposome-bound calcium by selective metal ions. Aliquots (5 μg each) of toposome were dot blotted onto nitrocellulose membrane and probed with ^{45}Ca as described in Materials and Methods Section.

bound ^{45}Ca with a competing ion (Fig. 5). Magnesium, Ba^{2+}, and Fe^{3+} were largely unable to displace Ca^{2+}. In contrast, both Cd^{2+} and Mn^{2+} effectively displaced Ca^{2+}. These results show that metal ions possessing an ionic radius similar to that of calcium, Cd^{2+}, and Mn^{2+}, can occupy the Ca^{2+}-binding sites on toposome while metal ions having an ionic radius much smaller or larger than that of calcium cannot occupy these sites, Mg^{2+}, Ba^{2+}, and Fe^{3+}. These results clearly indicate that the calcium-binding sites on toposome can selectively accommodate other divalent cations. However, these metal ions, Cd^{2+} and Mn^{2+}, are present in trace amounts in seawater, and therefore, are unable to interfere with the calcium-dependent functions of toposome. It is of interest to note that although magnesium is present in seawater at a concentration of 50 mM, it is excluded from the calcium-binding sites on toposome.

Recent research suggests that toposome is a transferrin-like iron binding protein and suggests that toposome transports free iron in the coelomic fluid to the testis and ovary, supporting gametogenesis [Brooks and Wessel, 2002]. As observed in the endogenous tryptophan fluorescence experiment (Fig. 4), toposome is capable of binding iron. Functional transferrins bind iron as Fe^{3+} with an extremely high affinity and are capable of transporting concentrations of iron at or below the nano-molar range [Baker et al., 2003]. However, our fluorescence data indicate that toposome has an apparent dissociation constant (Fe^{3+}) of 275 μM and appears to be insensitive to low concentrations of iron. Based on the apparent dissociation constant and the trace amounts of iron present in seawater, we suggest that toposome, although transferrin-like in sequence, is unlikely to function as an iron transporter in the developing sea urchin egg and embryo.

In conclusion, the results reported here further confirm and expand upon our knowledge of toposome structure and function. Thermal denaturation and chymotryptic digestion studies both provide further evidence for the two distinctive, Ca^{2+}-dependent structures of toposome. AFM confirmed our previous finding that the Ca^{2+}-dependent secondary structural change is necessary to facilitate toposome binding to the bilayer. In a previous study we showed that the Ca^{2+}-dependent tertiary structural change was required for toposome-driven, membrane–membrane interaction [Hayley et al., 2006a]. These data are significant in the context of the ability of sea urchin eggs and embryos to repair lesions in their plasma membranes. The patch hypothesis describes a two-step model in which yolk granules fuse in response to millimolar concentrations of Ca^{2+} and the resulting large vesicles then fuse with the damaged plasma membrane [Terasaki et al., 1997; McNeil et al., 2000]. Our previous data, supported by the results reported here suggest the intriguing possibility that toposome may be an important player on the pathway leading to plasma membrane repair. A lesion in the egg plasma membrane would result in an influx of seawater containing 10 mM Ca^{2+}. This Ca^{2+} would drive the tertiary structural change in toposome which in turn would drive membrane–membrane interaction. There are two possible models for defining a role for toposome in this process. The tertiary structural change may generate protein–protein interaction sites allowing toposome molecules on apposing membranes to interact. Alternatively, the tertiary structural change may expose a second membrane-binding site on toposome. This latter model precluded the necessity for toposome to be present on both interacting surfaces. We are presently designing experiments to distinguish between these models.

ACKNOWLEDGMENTS

This work was supported by grants from the Natural Sciences and Engineering Research Council of Canada, the Canada Foundation for Innovation and the Industrial Research and Innovation Fund (EM) and the Natural Sciences and Engineering Research Council of Canada (JJR).

REFERENCES

Baker HM, Anderson BF, Baker EN. 2003. Dealing with iron: Common structural principles in proteins that transport iron and heme. Proc Natl Acad Sci 100:3579–3583.

Brooks JM, Wessel GM. 2002. The major yolk protein in the sea urchin is a transferrin-like, iron binding protein. Dev Biol 245:1–12.

Cervello M, Di Ferro D, D'Amelio L, Zito F, Matranga V. 1992. Calcium-dependent self-aggregation of toposome, a sea urchin embryo cell adhesion molecule. Biol Cell 74: 231–234.

Gratwohl EKM, Kellenberger E, Lorand L, Noll H. 1991. Storage, ultrastructural targeting and function of toposomes and hyaline in sea urchin embryogenesis. Mech Dev 33:127–138.

Hayley M, Perera A, Robinson JJ. 2006a. Biochemical analysis of a Ca^{2+}-dependent membrane–membrane interaction mediated by the sea urchin yolk granule protein, toposome. Dev Growth Differ 48:401–409.

Hayley M, Emberley J, Davis PJ, Morrow MR, Robinson JJ. 2006b. Interaction of toposome from sea-urchin yolk granules with dimyristoyl phosphatidylserine model membranes: A ^{2}H-NMR study. Biophys J 91:4555–4564.

Hovis JS, Boxer SG. 2001. Patterning and composition arrays of supported lipid bilayers by microcontact printing. Langmuir 91:3400–3405.

Kari BE, Rottmann WL. 1980. Analysis of the yolk glycoproteins of the sea urchin embryo. J Cell Biol 87: 144a.

Laemmli UK. 1970. Cleavage of structural proteins during assembly of the head bacteriophage T4. Nature (London) 227:680–685.

Mallya SK, Partin JS, Valdizan MC, Lennarz WJ. 1992. Proteolysis of the major yolk glycoprotein is regulated by acidification of the yolk platelets in sea urchin embryos. J Cell Biol 117:1211–1220.

Matranga V, Kuwasaki B, Noll H. 1986. Functional characterization of toposomes from the sea urchin blastula embryos by a morphogenetic cell aggregation assay. EMBO J 5:3125–3132.

McNeil PL, Vogel SS, Miyake K, Terasaki M. 2000. Patching plasma membrane disruptions with cytoplasmic membrane. J Cell Sci 113:1891–1902.

Noll H, Matranga V, Palma P, Cutrono F, Vittorelli ML. 1981. Species-specific dissociation of live sea urchin embryos by Fab against membrane components of *Paracentrotus lividus* and *Arbacia lixula*. Dev Biol 87:229–241.

Noll H, Matranga V, Cervello M, Humphreys T, Kuwasaki B, Adelson D. 1985. Characterization of toposomes from sea urchin blastula cells: A cell organelle mediating cell adhesion and expressing positional information. Proc Natl Acad Sci 82:8062–8066.

Perera A, Davis P, Robinson JJ. 2004. Functional role of a high mol mass protein complex in the sea urchin yolk granule. Dev Growth Differ 46:201–211.

Robinson JJ. 1989. Selective metal ion binding at the calcium-binding sites of the sea urchin extraembryonic coat protein hyalin. Biochem Cell Biol 67:808–812.

Scott LB, Lennarz WJ. 1989. Structure of a major yolk glycoprotein and its processing pathway by limited proteolysis are conserved in echinoids. Dev Biol 132:91–102.

Terasaki M, Miyake K, McNeil PL. 1997. Large plasma membrane disruptions are rapidly resealed by calcium-dependent vesicle-vesicle fusion events. J Cell Biol 139: 63–74.

Yokota Y, Kato KH. 1988. Degradation of yolk granules in sea urchin eggs and embryos. Cell Differ 23:191–199.

Yokota Y, Unuma T, Moriyama A, Yamano K. 2003. Cleavage site of a major yolk protein (MYP) determined by cDNA isolation and amino acid sequencing in sea urchin, *Hemicentrotus pulcherrimus*. Comp Biochem Physiol B Biochem Mol Biol 135:71–81.